

# Posture standardization of pig point cloud based on skeleton extraction and transformation

Jimin Zhu<sup>1,2</sup>, Zhaoda Chen<sup>2</sup>, Ling Yin<sup>1,2,3\*</sup>, Gengyuan Cai<sup>1,3,5</sup>,  
Xiaochen Yao<sup>4</sup>, Sumin Zhang<sup>1,2,3</sup>, Huan Zhang<sup>5</sup>

(1. State Key Laboratory of Swine and Poultry Breeding Industry, Guangzhou, Guangdong 510640, China;

2. College of Mathematics Informatics, South China Agricultural University, Guangzhou 510642, China;

3. National Engineering Research Center for Swine Breeding Industry, Guangzhou 510642, China;

4. Guangdong Zhongxin Breeding Technology Co.,Ltd, Guangzhou 511458, China;

5. School of Foreign Studies, South China Agricultural University, Guangzhou 510642, China)

**Abstract:** Pig body measurement is an important evaluation criterion for breeding and production management. Automatic measurement algorithms for pig body sizes exhibit sensitivity to the point cloud posture, but non-standard pig postures may result in inaccurate joint point localization in body measurement, further affecting measurement accuracy and the commercial application of these algorithms. To address this challenge, this paper proposed a pig point cloud posture transformation method based on pig's skeleton model to adjust non-standard postures before conducting body size measurements. The method utilized an improved L1-median skeleton model to extract the three-dimensional skeleton of the pig point cloud, capturing the skeleton joint points on the target pig's head, body, and limbs. By binding the skeleton joint points with the local point cloud and using rotation matrices, non-standard postures were adjusted to standard ones, enabling accurate body size measurements. The experimental results demonstrated that the average relative errors between the transferred posture and the original standard posture were reduced to 0.89% in body length, 0.76% in body width (front), 1% in body width (back), 0.89% in body height (front), 1.7% in body height (back), 2.03% in thoracic circumference, 3.37% in abdominal circumference, and 1.89% in rump circumference. To conclude, the posture standardization transfer method can significantly reduce errors in important body size parameters such as body length, body height, and body width. The method displays a greater stability and robustness compared to existing posture normalization and regression adjustment methods, providing both guidance and insight for future research in intelligent agriculture.

**Keywords:** pig point cloud, body size measurement, posture transfer, skeleton extraction

**DOI:** [10.25165/j.ijabe.20251802.8644](https://doi.org/10.25165/j.ijabe.20251802.8644)

**Citation:** Zhu J M, Chen Z D, Yin L, Cai G Y, Yao X C, Zhang S M, et al. Posture standardization of pig point cloud based on skeleton extraction and transformation. Int J Agric & Biol Eng, 2025; 18(2): 63–74.

## 1 Introduction

Accurate body measurement can reflect the growth and development of livestock, estimate body weight, and assess body condition, facilitating genetic breeding and intelligent feeding management<sup>[1-4]</sup>. Traditional measurement methods rely on manual operation and require restraining animals in specific areas, which are not only time-consuming and inefficient but also prone to unnecessary stress responses of livestock<sup>[5,6]</sup>. Furthermore, manual measurement methods fail to meet the demands of large-scale livestock farms for batched, efficient, and continuous monitoring.

With the increasing demand for smart farming and precise

animal monitoring, depth cameras such as Kinect and RealSense have been successfully applied in the livestock industry<sup>[7-10]</sup>. In the process of automated body measurement, multiple-view depth cameras are first used to more efficiently capture three-dimensional data of livestock in standing or walking states. The data from different views are then reconstructed into a complete livestock model through target detection, extraction, registration, and fusion<sup>[11-14]</sup>. Key points for body size measurement are located using effective methods such as point cloud density distribution, geometric feature calculation, and part segmentation to obtain pig body length, body width, body height, and circumference parameters<sup>[15-17]</sup>. By utilizing ellipse fitting, point cloud segmentation, and curvature analysis, the body weight, surface area, and volume of animals are determined<sup>[7,18,19]</sup>, which are helpful in body condition scoring<sup>[20-22]</sup>.

During manual measurement of livestock body sizes, animals are required to maintain an ideal standard posture. Specifically, the head and tail of the pig should align in a straight line, with the limbs forming a rectangular stance. This posture facilitates monitoring from top, side, and leg point clouds, directly displaying the pig's primary body contours and structures. It minimizes measurement errors due to posture variations, ensuring consistency and accuracy of the data<sup>[23]</sup>. However, in actual measurements, even when restricted to a narrow measurement area, livestock tend to lower or raise their head, turn their head, and bend their body, resulting in various non-standard postures. Additionally, measurements in

Received date: 2023-11-12 Accepted date: 2024-12-03

**Biographies:** Jimin Zhu, MAg, research interest: precision agriculture, Email: [zhujimin@outlook.com](mailto:zhujimin@outlook.com); Zhaoda Chen, ME, research interest: image processing, Email: [2272689905@qq.com](mailto:2272689905@qq.com); Gengyuan Cai, PhD, Professor, research interest: pig breeding and production, Email: [cgy0415@163.com](mailto:cgy0415@163.com); Xiaochen Yao, MS, Researcher, research interest: pig breeding and production, Email: [YXC\\_enactus@163.com](mailto:YXC_enactus@163.com); Sumin Zhang, PhD, Professor, research interest: data mining, Email: [suminzhang@scau.edu.cn](mailto:suminzhang@scau.edu.cn); Huan Zhang, Master, Professor, research interest: translation teaching, Email: [346408697@qq.com](mailto:346408697@qq.com).

**\*Corresponding author:** Ling Yin, PhD, Professor, research interest: agricultural Information, smart farming and data mining. College of Mathematics Informatics, Engineering, South China Agricultural University, Guangzhou 510642, China. Tel:+86-13929587034. Email: [yin\\_ling@scau.edu.cn](mailto:yin_ling@scau.edu.cn).

different postures may bring about different body sizes. Experimental results indicate that the proportion of standard postures is only 25% in the actual data acquisition (those accurately reflecting the pig's actual body sizes), while 75% represent non-standard postures, introducing a considerable level of uncertainty into body size measurements<sup>[24]</sup>. Therefore, to ensure accuracy in manual measurements, the average values of body parameters from multiple measurements on the same animal are often taken. The results of manual measurements are subjective and influenced by non-standard postures, making them unreliable as the gold standard for true body measurements.

Different postures can affect the accuracy of body measurements. For instance, compared to the standard posture of a pig, when the head tilts more towards the ground, the body length tends to increase, the front height diminishes, and measurements like abdominal girth and chest girth tend to be larger. Moreover, increased body twisting amplitude corresponds to longer body length, which can also affect body width. Ling et al. show that point cloud postures of livestock collected in free-walking states are diverse, with only a quarter of the data representing the standard posture<sup>[24]</sup>. Compared with manual measurement, the automatic measurement method of standard posture, and the error of body length, body width, body height, and abdominal circumference in non-standard posture, the maximum error can reach 10%. The previous research aimed to improve the accuracy of livestock body size measurement by quantifying the relationship between the vector set of skeleton joint points and body sizes and applying a regression model to calibrate the body size data. Another approach involves fitting point cloud data with statistical three-dimensional

models of animals and normalizing the point cloud postures through methods such as estimating the animal's forward direction, segmenting point cloud of body parts, bilateral symmetry, and posture normalization<sup>[25,26]</sup>. However, this method requires high-precision three-dimensional models for each type of livestock and significant computational costs<sup>[27]</sup>. Automated measurement of livestock body sizes should be conducted in the standard posture, as direct measurements in non-standard postures can lead to considerable errors. Therefore, posture correction of livestock point clouds is crucial. In this study, we present a method for posture standardization transfer and body size measurement based on a pig skeleton model, which is marked by transforming non-standard postures to a standard posture before conducting body size measurements.

The main contributions of this paper are as follows:

(1) Improving the L1-median skeleton model to accurately extract the three-dimensional point cloud skeleton of pigs.

(2) Introducing a point cloud posture standardization transfer method based on skeleton joint points, which enables the livestock point clouds in non-standard postures to transfer to a standard posture.

## 2 Materials and methods

Extraction of the 3D skeleton model and skeleton joint points from complete pig body point cloud data makes posture standardization transfer feasible. Meanwhile, comparative measurements can also be realized, such as body length, body height, thoracic circumference, abdominal circumference, and rump circumference. The specific process is shown in Figure 1.

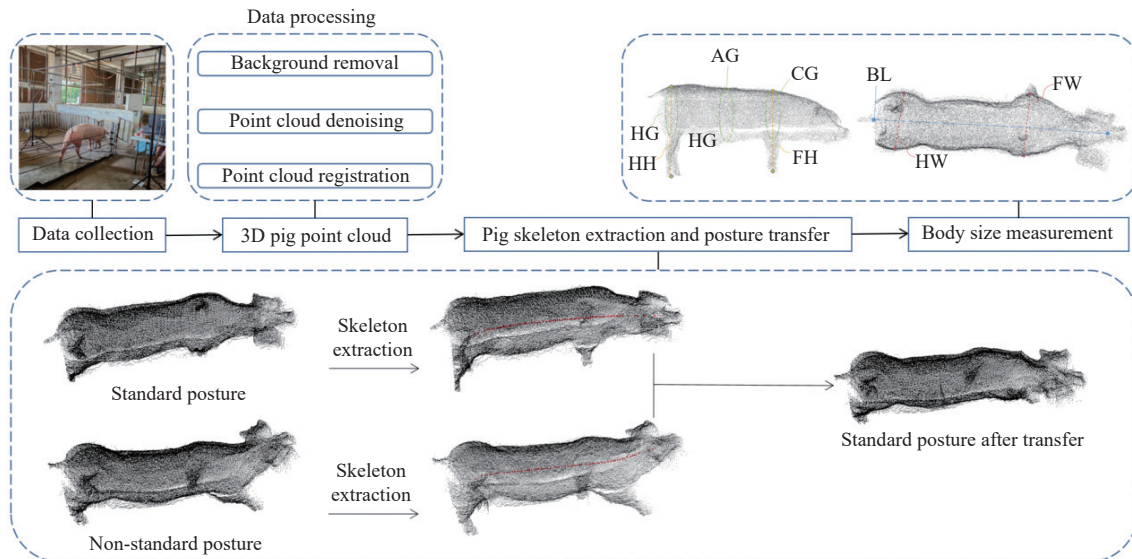


Figure 1 Specific process of pig posture transfer and body measurement

### 2.1 Data preprocessing

All procedures in this experiment were approved by the laboratory Animal Ethics Committee of South China Agricultural University (reference number 2020G008). The data for this experiment were collected from July 1 to August 1, 2022, at Wens Foodstuff Group Co., Ltd. in Heyuan City, Guangdong Province. Depth cameras in three directions were used to capture local point cloud data, and after registration, denoising, and downsampling, complete pig body point clouds in different postures were obtained. For detailed information on the data acquisition process and the specific definitions of different pig postures, please refer to our previous studies<sup>[24,28]</sup>.

### 2.2 Pig skeleton model

A three-dimensional skeleton can describe the geometric topology of a pig, providing an intuitive and comprehensible representation. Similarly, a pig skeleton model can assist in posture classification and posture transfer. Due to limitations in camera perspectives and factors such as strong sunlight, incomplete point cloud data or uneven distribution of local point clouds may be found in the front or hind legs of a target pig. Directly applying the L1-median skeleton extraction algorithm cannot accurately describe the shape of the pig body<sup>[29]</sup>. Therefore, in this paper, an improved local L1-median skeleton extraction algorithm is employed to describe the shape features of the pig body with more accuracy.

### 2.2.1 Pig skeleton extraction

In our experiment, the pig skeleton point cloud is acquired by randomly sampling the input point set  $Q = \{q_j\}_{j \in J} \subset \mathcal{Q}^3$  to obtain a sparse point set  $X = \{x_i\}, i \in I \subset \mathcal{Q}^3$ , determining the local centers of points within the neighborhood, and gradually expanding the neighborhood range. The point cloud data of a pig skeleton can be ultimately obtained:

$$\operatorname{argmin}_x \sum_{i \in I} \sum_{j \in J} \|x_i - q_j\| \theta(\|x_i - q_j\|) + R(X) \quad (1)$$

where, the first part determines the local L1-median, which obtains the central points of the local point cloud.  $I$  and  $J$  index the set of points  $X$  and points  $Q$ , respectively. The parameter  $\theta(r) = e^{-\|r\|^2/(h/2)^2}$  is the Gaussian weight function of the initial radius  $h$ . The weight is lower in high-density regions to generate effective skeleton branches;  $r$  is the Euclidean distance between point  $x_i$  and point  $q_j$ , allowing the skeleton extraction algorithm to adaptively process point cloud regions with different density levels. The term  $R(X)$  is introduced as a regularization function that adjusts the repulsive force of the skeleton points to maintain sparsity, while the weight is greater in low-density regions to make the skeleton closer to the true shape.

$$R(X) = \sum_{i \in I} \gamma_i \sum_{i' \in I \setminus \{i\}} \frac{\theta(\|x_i - x_i'\|)}{\sigma_i \|x_i - x_i'\|} \quad (2)$$

where,  $\gamma_i$  is the parameter that balances gravity and repulsive forces; and  $\sigma_i$  is used to differentiate between skeleton points and non-skeleton points.  $\sigma_i = \frac{\lambda_2^i}{\lambda_0^i + \lambda_1^i + \lambda_2^i}$ , represents the concentration of the point cloud in a local region, and  $\lambda_0^i, \lambda_1^i, \lambda_2^i$  is the extent of stretch in different directions at that point. The closer the parameter is to 1, the greater the concentration of the point cloud along the direction  $\lambda_2$ , resulting in a line-like distribution. When handling irregular and incomplete point cloud data, enhancing the accuracy and stability of skeleton extraction makes it more likely that the skeleton point is located on a skeleton branch.  $x_i'$  represents the points adjacent to  $x_i$ .

### 2.2.2 Skeleton optimization

Extracting the L1-median skeleton heavily relies on surface points. When the distribution of surface points on the pig body is uneven, the extracted local skeleton tends to be concentrated in regions where surface points are relatively dense. To achieve a uniform distribution of skeleton points and form a complete and consistent pig body skeleton model, density weighting is applied to initial pig skeleton optimization. This involves quantifying the point cloud density in local regions to obtain density weights for the skeleton points, which are formulated as follows:

$$d_j = 1 + \sum_{i' \in I \setminus \{i\}} \theta(r) \quad (3)$$

$$\alpha_{ij}^k = \frac{\sum_{j \in J} q_j \alpha_{ij}^k / d_j}{\sum_{j \in J} \alpha_{ij}^k / d_j} + \mu \sigma_i^k \frac{\sum_{i' \in I \setminus \{i\}} (x_i^k - x_{i'}^k) \beta_{ii'}^k}{\sum_{i' \in I \setminus \{i\}} \beta_{ii'}^k} \quad (4)$$

where,  $d_j$  denotes the weighted local density of  $r$ , which is used to regulate the local density between point  $x_i$  and point  $q_j$ .  $\alpha_{ij}^k = \frac{\theta(\|x_i^k - q_j\|)}{\|x_i^k - q_j\|}$  is the angular discrepancy between point  $x_i$  and point  $q_j$ , which contributes to calculating the repulsive force between the two points. Meanwhile,  $\beta_{ii'}^k = \frac{\theta(\|x_i^k - x_{i'}^k\|)}{\|x_i^k - x_{i'}^k\|^2}$  signifies the

attractive force between these points,  $k$  indicates the iteration count, and  $\sigma_i^k = \sigma(x_i^k)$ .

Furthermore, pig point clouds often have small missing portions, and the generated L1-median skeleton may deviate from these missing parts, thus affecting the overall structure of the skeleton. This paper introduces an ellipse fitting approach, which finds an ellipse that minimizes the distance between known point clouds and the ellipse to approximate the missing surface point cloud<sup>[30]</sup>. The formula for ellipse fitting is as follows:

$$F(a, x) = \mathbf{ax} = ax^2 + bxy + cy^2 + dx + ey + f = 0 \quad (5)$$

where, the parameter vector  $\mathbf{a} = [a, b, c, d, e, f]^T$  and the coordinate vector  $\mathbf{x} = [x^2, xy, y^2, x, y, 1]^T$  are used. For a point  $(x_i, y_i)$ ,  $F(a, x_i)$  represents the algebraic distance from the point to the curve  $F(a, x) = 0$ .

By applying density weighting optimization and ellipse fitting to the pig skeleton model, the generated skeleton points not only exhibit a uniform distribution but also provide a complete description of the pig contour.

### 2.3 Posture standardization transfer

There are significant differences in body length, body width, body height, abdominal circumference, and other measurements between pigs in non-standard postures and pigs in standard postures. In real scenarios, various point cloud postures are collected in a pig's free-walking state, which can affect the accuracy and stability of body size measurements. To reduce measurement errors caused by posture variations, this study proposes a method to adjust non-standard postures to standard postures.

#### 2.3.1 Skeleton joint extraction

The skeleton of a pig is divided into four parts: head, torso, front legs, and hind legs. As a definition of pig skeleton in a strict biological sense is not yet available, this study utilizes 32 skeleton joint points from the pig skeleton that represent the main physiological structures of the pig's hoof. As shown in Figure 2, three joint points are uniformly obtained from the pig's head, 17 joint points from its torso, and 12 joint points from its front and hind legs, totaling 32 joint points on a pig skeleton. The purpose of selecting these nodes is to ensure a uniform distribution of data across each part of the skeleton, which aids in accurately identifying standard postures and enhancing the precision of body size measurements.

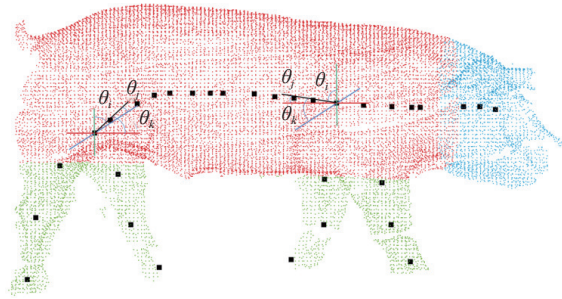


Figure 2 32 joint points of pig skeleton

The joint points from the head and torso of a pig are arranged in ascending order along the  $x$ -axis to establish the coordinate system for the  $i^{th}$  joint point, denoted as coordinate system  $g_i = \{x_i, y_i, z_i\}$ . The collection of joint points from the head and body  $G = \{g_1, g_2, \dots, g_k\}$ ,  $k = 20$ , comprising 20 joints from the pig's head to its hindquarters, constructs a vector denoted as  $v_{i,i+1}$ , which can be calculated by Equation (6):

$$v_{i,i+1} = \{g_{i+1} - g_i | i = 1, 2, \dots, K-1\} \quad (6)$$

### 2.3.2 Skeleton joint weight binding

To achieve posture standardization transfer, the skeleton joint points of the pig are selected as the central points of the local point cloud. The skeleton joint points can represent the important geometric features of the local point cloud, such as the pig body contour and the pig posture, which are crucial for posture standardization transfer.

Based on the distance between the skeleton joints and the surface point cloud of the pig body, the points within a certain distance from the skeleton joints in the local point cloud are bound to their corresponding joints. As shown in Figure 3, each skeleton joint serves as the center of a sphere, where the surface of the sphere represents the distribution of the pig body surface point cloud around that joint.  $c_0$  is the coordinates of the skeleton joint points,  $p$  represents the pig body surface point cloud, and  $r_0$  represents the distance between the skeleton joint points and the surface point cloud. Figure 3a illustrates the ideal relationship between the skeleton joint points and its associated local point cloud. Assuming there are  $M$  ( $M \geq 2$ ) point clouds on the sphere,  $M$  points are evenly distributed along the edge of the circle and are closest to point  $c_0$ . The distance from these points to the center  $c_0$  is equal to the radius of the sphere  $r_0$ , which can be expressed as:

$$d(p_i, c_0) = r_0 \text{ for } i = 1, 2, \dots, M \quad (7)$$

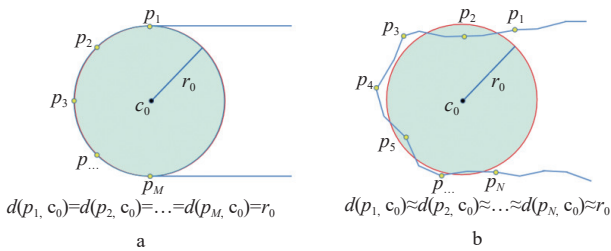


Figure 3 Illustration of radius calculation using the nearest distance

In Figure 3b, the situation is more realistic, where there is noise on the surface and the pig body surface point cloud  $p$  is haphazard and not entirely located on the edge of the sphere. In this case, given a set of  $M$  points, a combination of weights  $\{w_1, w_2, \dots, w_M\}$  is used for any arbitrary convex combination to obtain the nearest distance. The weights for point clouds closer to the skeleton joint point  $c$  have larger values, while those farther from  $c$  have smaller values, even zero. The skeleton point  $c$  is approximated as a convex

combination of the input local point cloud that is closer to  $c$ . Therefore, through the same combination weights, the weighted average of the nearest distances is used as an approximation of the radius to obtain a reasonable estimation of the true radius. The sphere radius can be calculated as:

$$\sum_{i=1}^M w_i d(p_i, c_0) = r_0 \text{ with } \sum_{i=1}^M w_i = 1 \quad (8)$$

Combining the two scenarios mentioned above, the farthest distance from point  $p$  to all skeleton joints  $c_i$  is defined as:

$$d(p, \{c_i\}) = \min_{c \in \{c_i\}} \|p - c\|_2 \quad (9)$$

When the distance between point  $p$  and the skeleton joint point  $c_i$  is less than the radius  $r_0$ , the point is considered part of the local point cloud and is bound to the skeleton joint point. If the distance is greater than  $r_0$ , the point is not considered part of the local point cloud and will not be bound to the skeleton joint point. In the case where a point cloud is close to two adjacent skeleton joint points, according to the nearest neighbor principle, the point cloud is bound to the skeleton joint point that is closest in distance, indicating a stronger association with the nearest skeleton joint point. With the above method, the complete pig point cloud data can be divided into 20 local point cloud datasets  $P_i$  by the 20 skeleton joint points on a pig torso. Each local point cloud corresponds to one skeleton joint point and reflects the shape features around that joint point.

### 2.3.3 Posture standardization transfer and local point cloud rotation

To extract posture information from skeleton joint points, we first establish a collection of vector angles for standard and non-standard postures of each target pig. This collection primarily focuses on the skeleton joint points of the head and trunk, excluding the legs. We define the vector angle set  $V_{\text{norm}}$  for standard postures and the vector angle set  $V_{\text{pose}}$  for non-standard postures, forming local vector angles  $\theta_i$ ,  $\theta_j$ , and  $\theta_k$  with planes  $XOZ$ ,  $XOY$ , and  $YOZ$ , respectively. The vector angle sets are formulated as follows:

$$V_{\text{norm}} = \{v_{\text{norm}, i} | v_{\text{norm}, i} = (\theta_i, \theta_j, \theta_k) \text{ for } i = 1, 2, \dots, k-1\} \quad (10)$$

$$V_{\text{pose}} = \{v_{\text{pose}, i} | v_{\text{pose}, i} = (\theta'_i, \theta'_j, \theta'_k) \text{ for } i = 1, 2, \dots, k-1\} \quad (11)$$

where,  $K$  represents the skeleton joint points of the trunk and head, totaling 20 joint points. Figure 4 shows the vector angles of the skeleton joint points for standard and non-standard postures.

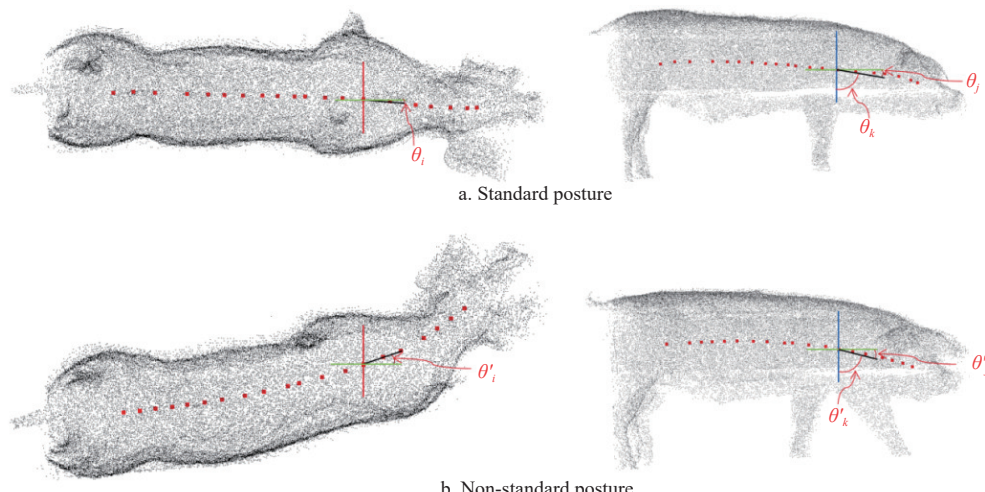


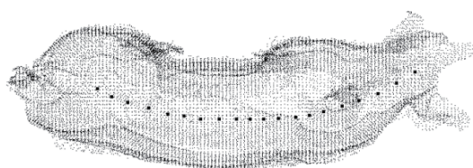
Figure 4 Comparison of vector angles for pig postures

The objective of this study is to transfer the non-standard posture of pigs to the standard posture, which cannot construct a fixed or uniform collection of skeleton joint vectors. In previous research, Ling et al. discovered that pig skeleton joint vectors can be used for posture classification<sup>[24]</sup>. For instance, when a pig lowers its head, arches its back, or twists its body, the vector angles of these postures are significantly larger than those of standard postures. Based on the skeleton joint vectors, pig postures can fall into two categories: standard postures and non-standard postures. However, given biological dynamic variations, the standard posture of any individual pig is unique, and the vector angles of non-standard postures may not precisely reach the ideal target values of standard postures. Therefore, in the preprocessing phase, all point cloud data of each pig are first classified as standard postures and non-standard postures. After normalizing the vector angles of the skeleton joint points to the range [0, 1], a standard posture threshold range for each skeleton joint point is set, with thresholds of 0.1 for the head and 0.03 for the trunk. These threshold ranges serve as references for the standard posture, while the vector angles of the head and trunk for non-standard postures are greater than the threshold ranges. Provided that all the vector angles of the transferred skeleton joint points fall within the threshold ranges of the reference standard posture, the pig point cloud data is considered to have approached and transferred to the standard posture.

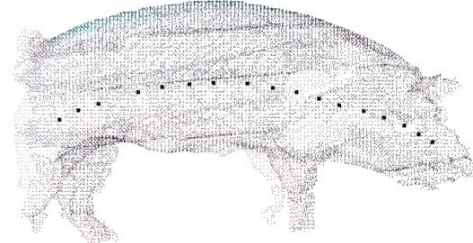
First, the corresponding rotation matrices are calculated based on each pair of vector angles of the skeleton joint points. These rotation matrices are then applied to the respective local point clouds of non-standard postures, resulting in rotated local point clouds denoted as  $R_x(\theta)$ ,  $R_y(\delta)$ , and  $R_z(\gamma)$ , respectively:

$$R_x(\theta) = \begin{bmatrix} 1 & 0 & 0 \\ 0 & \cos\theta & -\sin\theta \\ 0 & \sin\theta & \cos\theta \end{bmatrix} \quad (12)$$

$$R_y(\delta) = \begin{bmatrix} \cos\delta & 0 & \sin\delta \\ 0 & 1 & 0 \\ -\sin\delta & 0 & \cos\delta \end{bmatrix} \quad (13)$$



a. Before posture standardization transfer (top view)



c. Before posture standardization transfer (side view)

$$R_z(\gamma) = \begin{bmatrix} \cos\gamma & -\sin\gamma & 0 \\ \sin\gamma & \cos\gamma & 0 \\ 0 & 0 & 1 \end{bmatrix} \quad (14)$$

where,  $\theta = |\theta'_i - \theta_i| < \varepsilon$ ,  $\delta = |\theta'_j - \theta_j| < \varepsilon$ ,  $\gamma = |\theta'_k - \theta_k| < \varepsilon$ ,  $\theta_i$ , and  $\theta'_i$  represent the vector angles of the  $i^{\text{th}}$  skeleton joint points for standard postures or non-standard postures, and  $\varepsilon$  represents the threshold value of the vector angles for standard postures. The three rotation matrices are multiplied to obtain the total rotation matrix denoted as  $R$ :

$$R = R_x(\theta) \times R_y(\delta) \times R_z(\gamma) = \begin{bmatrix} \cos\delta\cos\theta & \sin\gamma\sin\delta\cos\theta - \cos\gamma\sin\delta & \cos\gamma\sin\delta\cos\theta + \sin\gamma\sin\theta \\ \cos\delta\sin\theta & \sin\gamma\sin\delta\sin\theta + \cos\gamma\cos\theta & \cos\gamma\sin\delta\sin\theta - \sin\gamma\cos\theta \\ -\sin\delta & \sin\gamma\cos\theta & \cos\gamma\cos\theta \end{bmatrix} \quad (15)$$

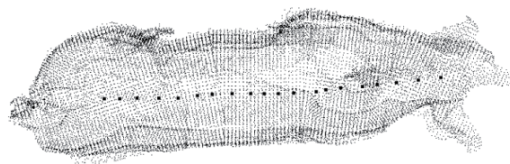
The rotation matrix  $R$  is applied to the corresponding local point cloud  $P_i$  of the non-standard posture, generating a new rotated local point cloud denoted as  $P_j$ :

$$P_j = R \times P_i \quad (16)$$

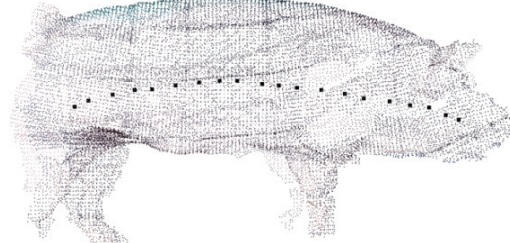
To ensure the continuity between adjacent local point clouds during the transfer process, the lengths of the skeleton joint points between the original local point clouds are calculated. These lengths are maintained unchanged during the rotation process to prevent any pig body discontinuities. Finally, the rotated local point clouds are connected in the sequential order of the skeleton joints, forming a complete transferred standard posture of pigs, as shown in Figure 5.

### 2.3.4 Evaluation metrics

This study utilizes evaluation metrics to assess the feasibility of posture transfer. Due to the unordered nature of point clouds, Chamfer Distance (CD) and Mean Absolute Error (MAE) are commonly used as evaluation methods to measure the error between the transferred non-standard posture and the original standard posture. CD calculates the average distance between the points of the transferred point cloud  $S_1$  and the point cloud of the original standard posture  $S_2$ , while MAE reflects the overall error level during the transfer process.



b. After posture standardization transfer (top view)



d. After posture standardization transfer (side view)

Figure 5 Comparison before and after posture standardization transfer

#### (1) Chamfer distance (CD):

$$d_{\text{CD}}(S_1, S_2) = \frac{1}{S_1} \sum_{x \in S_1} \min_{y \in S_2} \|\mathbf{x} - \mathbf{y}\|_2 + \frac{1}{S_2} \sum_{y \in S_2} \min_{x \in S_1} \|\mathbf{x} - \mathbf{y}\|_2 \quad (17)$$

where,  $x$  and  $y$  represent the 3D coordinates of respective point

clouds. A smaller CD value indicates a smaller difference between the transferred point cloud  $S_1$  and the reference point cloud of the standard posture  $S_2$ . However, CD is a global metric that only considers the distance between points and does not take into account the correspondence between point clouds. Therefore, it is

combined with mean absolute error (MAE) to comprehensively evaluate the accuracy in the posture standardization transfer.

(2) Mean absolute error (MAE):

$$MAE = \frac{1}{N} \sum_{i=1}^N |s_1 - s_2| \quad (18)$$

where,  $N$  represents the number of points in the point cloud. For each point  $s_1$  in the point cloud  $S_1$ , the nearest neighboring point  $s_2$  in the point cloud  $S_2$  is found, and the distance is calculated to obtain MAE. A smaller MAE value indicates higher accuracy in posture standardization transfer, suggesting better correspondence between the point clouds  $S_1$  (the transferred posture) and the reference point cloud  $S_2$  (the standard posture).

### 3 Results and analysis

The experimental subject in this study was Landrace pigs whose body weight ranged from 80 to 140 kg. A total of 739 sets of point cloud data from 96 pigs were collected, with each target pig providing at least three sets of complete 3D point cloud data, including at least one set in standard postures and several sets in non-standard postures. In addition, the point cloud data of each pig were classified into standard posture and non-standard posture. By extracting the skeletal model from the pig body point cloud and manipulating the skeleton joint points, posture standardization transfer was performed and eventually the body sizes of the pigs were calculated.

#### 3.1 Skeleton extraction results

A complete skeleton structure of a pig consists of a trunk branch and four leg branches. Direct application of the  $L_1$ -median skeleton extraction method can generate skeleton extraction, as shown in Figure 6. In the pig point cloud data in our experiment, there were missing regions along the abdominal contour line, and these missing regions could not generate a particular part of the skeleton, causing discontinuity in the connection regions between the limbs and the trunk (Figures 6a-6f). Moreover, when the front legs or the hind legs of a pig were too close to each other, or when the legs were raised or bent, the point clouds interfered with each other, resulting in only one skeleton branch that did not match the actual topology of the pig (Figures 6b-6d). In addition, the high density of point cloud in the head and ear regions led to a chaotic extraction of the skeleton, failing to accurately describe the shape of the pig (Figure 6e).

An improved skeleton extraction algorithm has been applied in this research, as shown in Figure 7. First, the missing points along the abdominal contour line were repaired using ellipse fitting, thus eliminating the missing regions and ensuring the correct connection between the trunk branch and the leg branches (Figures 7a-7c). What is more, in regions with dense point cloud such as the legs and the head, local point cloud density quantization was performed, ensuring the accurate generation of skeleton branches for the legs and the head. Accordingly, the accuracy and integrity of the skeleton was improved, and the topology and morphology of the pig was precisely described (Figures 7d-7f).

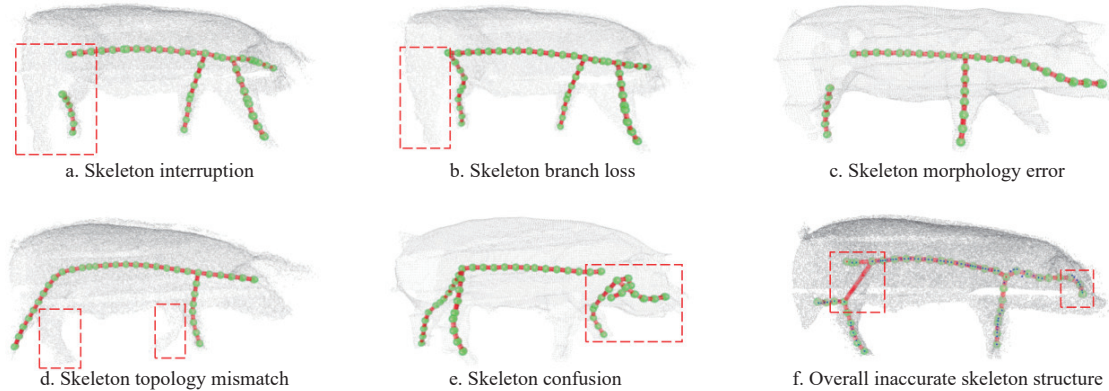


Figure 6 Incorrect skeleton extraction

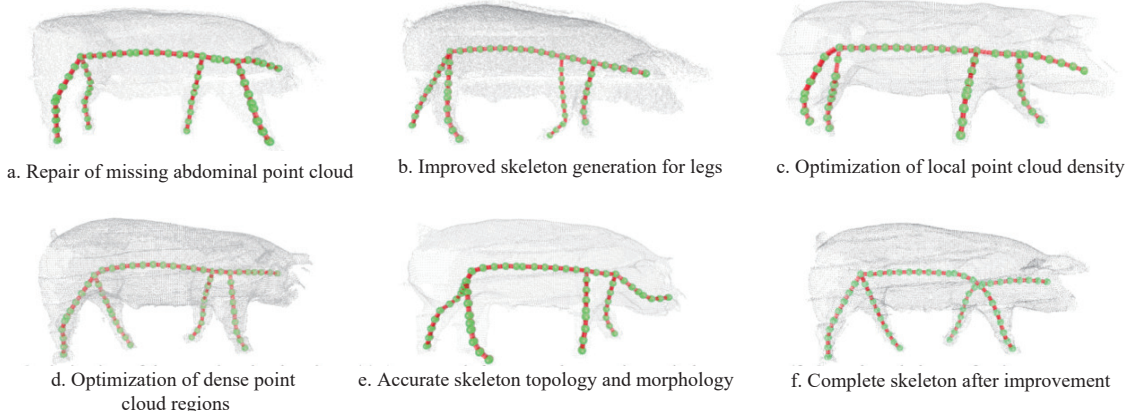


Figure 7 Visualization of improved skeleton extraction

#### 3.2 Posture standardization transfer results

The posture transfer of pigs involves the transfer of various non-standard postures. Based on the results of pig skeleton extraction, it

is necessary to integrate the accurate pig skeleton into the process of pig posture transfer to ensure the reliability and feasibility of posture transfer.

Figures 8-11 show the results of transferring non-standard postures to standard postures, including the initial non-standard postures, the transferred postures, and the standard postures. The skeleton joint points are marked with red dots. As shown in Figures 8 and 9, the non-standard L-shaped posture (Figure 8a) and C-shaped posture (Figure 9a) were so successfully transferred that they basically resembled the standard posture shown in Figure 9c. The

skeleton joint point vector angles from the pig's rump, trunk, and head remained within a specific threshold range of the standard posture, and the skeleton joint points translated to accurate position in the point cloud. This concordance in the contour of the torso with that of the standard posture indicated that the source posture was effectively transferred to a standard pose, with the pig's head, body, and tail aligned in a straight line.

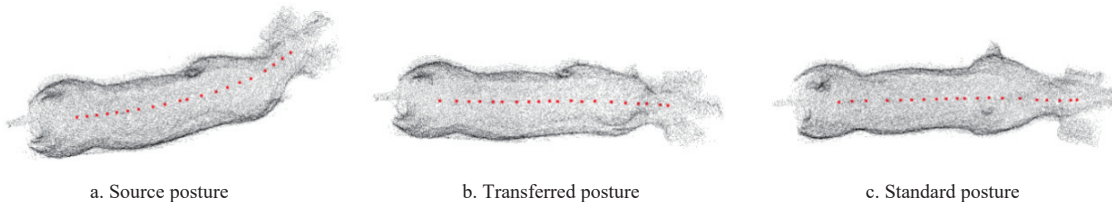


Figure 8 Comparison of standardization transfer results (L-shaped posture)

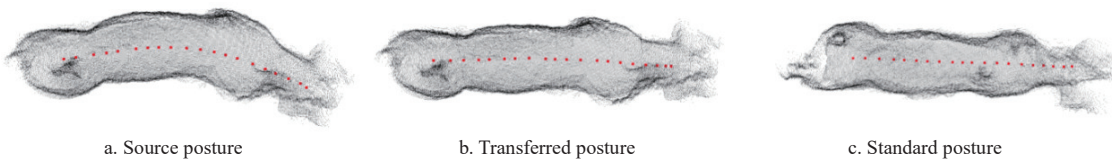


Figure 9 Comparison of standardization transfer results (C-shaped posture)

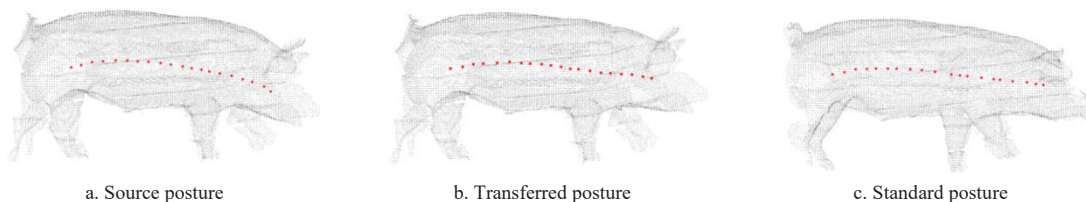


Figure 10 Comparison of posture standardization transfer results (lowering head)

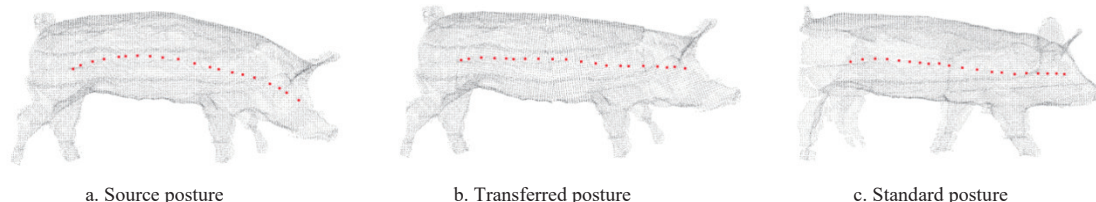


Figure 11 Comparison of head posture standardization transfer results (excessively lowering head)

In Figures 10 and 11, non-standard postures with different degrees of lowering the head were transferred to a standard posture with level eyes. Different degrees of head lowering in non-standard postures lead to varying degrees of stretching in the point clouds of the back and abdomen. As the pig's head lowers further, more point clouds are observed in the back and abdomen. During the transfer process, not only the head posture was regulated, but the entire trunk was also adjusted to the posture marked by looking straight ahead. It is worth noting that the legs had a minimal influence on the overall posture during the posture classification and transfer, so no specific adjustments were made to the legs during the transfer. Although the skeleton joint point positions of the legs are fixed during the posture transfer, the variations in the trunk point cloud of the pig result in corresponding changes in the key points used to measure body width, body height, girth, and other parameters. Therefore, even though no specific adjustments are made to the legs, they still affect the measurement results of body sizes.

In this study, CD and MAE were used to make comparisons between the transfer results of five types of non-standard postures (L-shaped, C-shaped, slightly lowering head, lowering head, and

excessively lowering head) and the reference standard posture. The results are listed in Table 1.

Table 1 Evaluation results of CD and MAE for the transfer of five types of non-standard postures

Non-standard posture	CD/cm	MAE before standardization transfer/cm	MAE after standardization transfer/cm
L-shaped	0.651	1.867	0.538
C-shaped	0.728	2.738	1.165
Slightly lowering head	0.549	1.435	0.703
Lowering head	0.685	3.355	1.173
Excessively lowering head	0.831	5.446	1.409
Average	0.689	2.968	0.998

The first column of the table presents the evaluation results of CD. In all five types of non-standard postures, the CD values were within a small range, with an average CD of 0.689. This shows that the transferred point clouds generally had insignificant difference compared to the reference posture point clouds, indicating a high degree of overall alignment between the point clouds. The second

and third columns represent the MAE between the point clouds before and after posture standardization transfer and the reference posture point clouds. In most postures, the MAE after standardization transfer was reduced compared to that before standardization transfer, indicating an improvement in most point clouds during the transfer process. The transferred point clouds matched the reference posture point clouds more accurately, suggesting more resemblance. However, for postures with obvious changes such as the C-shaped posture, lowering head, and excessively lowering head, the MAE after standardization transfer remained relatively large, reaching 1.165, 1.173, and 1.409, respectively. The main reason for the large MAE is not the failure to transfer to the ideal standard posture but rather issues such as matching errors between the point clouds because of different coordinate systems, different numbers of point clouds, and other factors (Figure 12).

In Figure 12a represents the raw data before processing, where each dataset is in a separate coordinate system. Challenges such as missing point cloud and noise can occur, making it difficult to accurately measure errors by aligning all the data of each pig in the same coordinate system. Therefore, in the evaluation process, errors should be minimized. The evaluation metrics, namely CD and MAE, remained within an acceptable range, demonstrating the robustness and effectiveness of the proposed posture standardization transfer method despite incomplete and noisy data.

In this process, accurate pig skeleton extraction and integration into the posture transfer process ensure the effective and accurate transfer of non-standard postures to standard postures. Both the pig's skeleton joint points and point cloud are effectively located and transferred. This step ensures the effectiveness and accuracy of posture transfer.

### 3.3 Body size measurement results

The posture standardization transfer results in this study have been validated by different body size measurement algorithms. Figure 13 is the body length measurement algorithm proposed by

Hao et al.<sup>[15]</sup>, which is based on PointNet++ for pig body part segmentation. Figure 13a shows the body length fitting results for non-standard postures, while Figure 13b shows the body length fitting results after transferring to a standard posture.

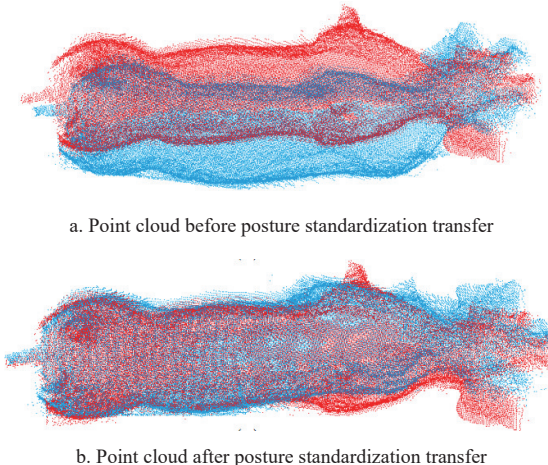


Figure 12 Comparisons of posture standardization transfer (Area in red: standard posture; area in blue)

When the pig is in a non-standard posture, such as lowering its head (Figure 14b), the skin of the pig undergoes stretching. Consequently, this impacts the calculation of body length and girth, leading to an increased density of point clouds in the dorsal and ventral regions. Concurrently, this also results in suboptimal localization of key points and curve fitting, causing recorded values to surpass those obtained in standard postures for parameters like body length and girth. Nevertheless, upon transferring the pig to a standard posture (Figure 14a), there is a notable enhancement in the positioning of key points and curve fitting, yielding more precise measurement outcomes. Hence, it is imperative to transition pigs from non-standard postures to standard postures to uphold measurement accuracy.

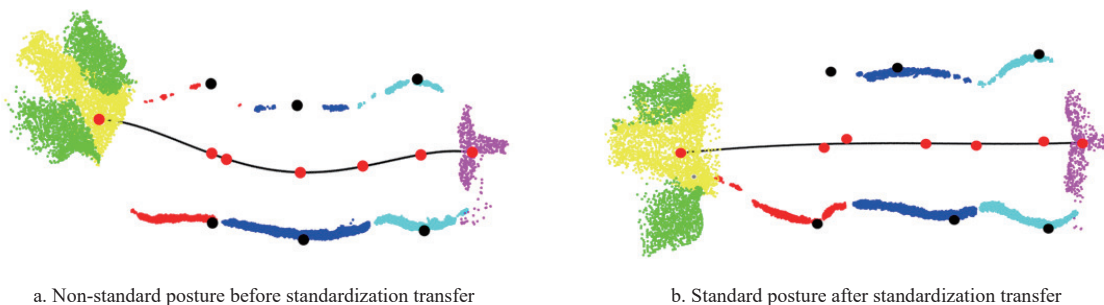


Figure 13 Body length measurement results

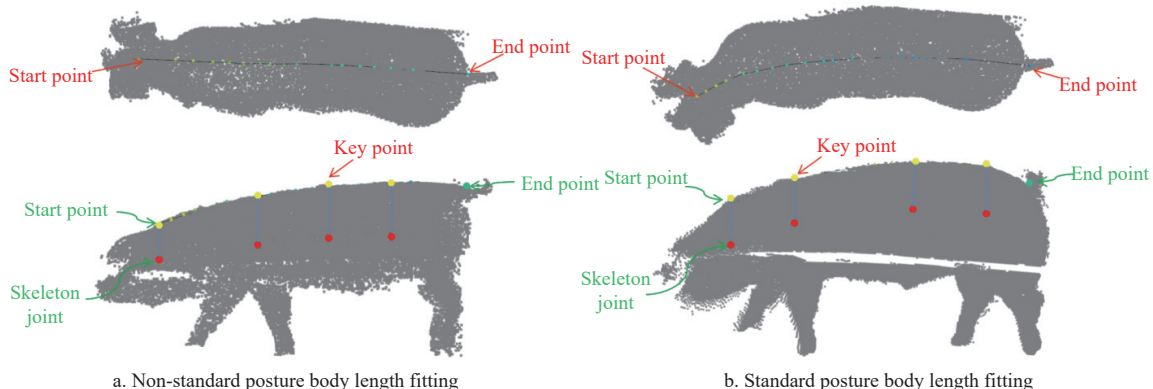


Figure 14 Body length measurement results before and after posture standardization transfer

Figure 14 demonstrates the application results of the body size measurement algorithm proposed by Yin et al.<sup>[16]</sup>, revealing the body length fitting results for non-standard and standard postures (Figures 14a, 14b). It can be observed that the localization of key points and curve fitting were significantly improved in standard postures compared to non-standard postures.

Due to the different shapes of the non-standard posture point clouds, deviations can be found in the measurement positions of body width (BW) compared to the standard posture (Figure 15a).

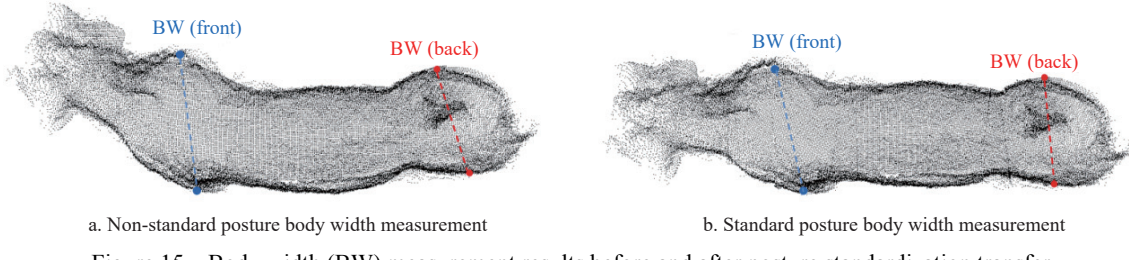


Figure 15 Body width (BW) measurement results before and after posture standardization transfer

Figure 16 illustrates the differences in body size measurements between the nose-down posture (Figure 16a) and the head-up posture (Figure 16b). In the nose-down posture, the pig's body (front) arches and tilts downward, leading to underestimated measurement results in body height (front) and thoracic circumference, as well as overestimated measurement results in

However, after transferring a non-standard posture to a standard posture (Figure 15b), the localization of key points and measurement positions for body width (BW) can be restored to the correct positions. Although the skeletal joint point positions of the legs are irrelevant, the overall changes in the point cloud of the trunk result in differences in the localization of surface key points. When calculating parameters that involve the straight-line distance between two points on the torso, the shape and posture of the entire pig body point cloud are taken into consideration.

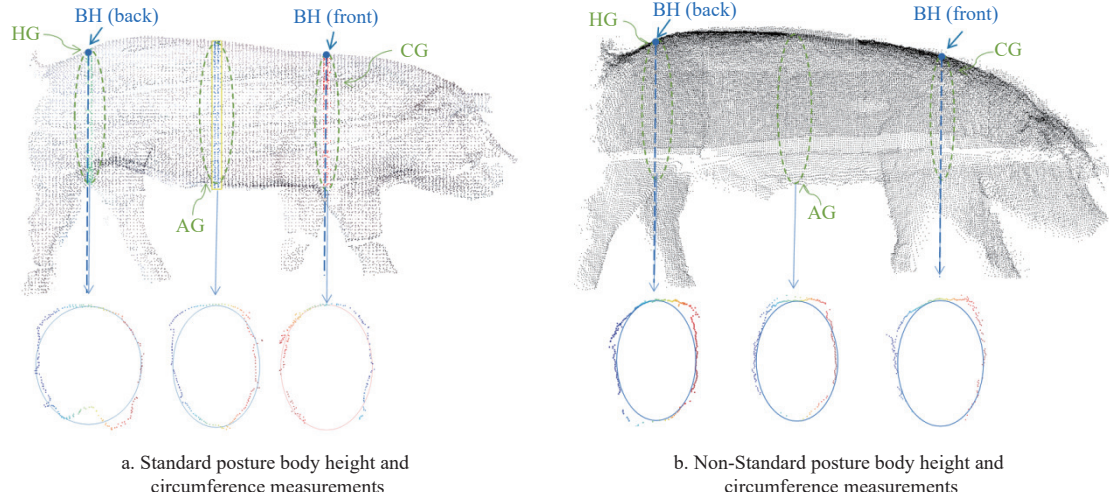
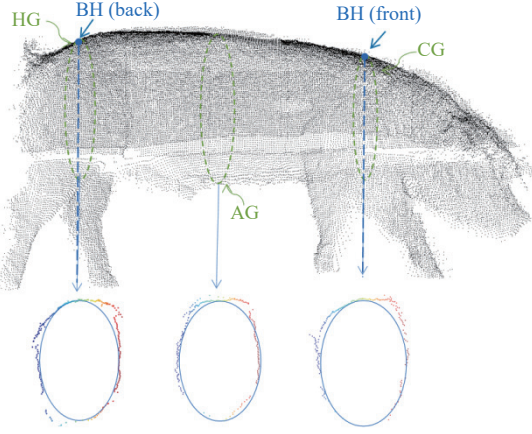


Figure 16 Measurement results of body height (BH), thoracic circumference (TC), abdominal circumference (AC), and rump circumference (RC) before and after posture standardization transfer

The pig body size was measured using the body size measurement algorithm proposed by Hao et al.<sup>[15]</sup> Figure 17 shows the contrast between the transferred postures and the original standard posture before and after posture standardization transfer in terms of relative errors, including body length (BL), body width (front), body width (back), body height (front), body height (back), thoracic circumference (TC), abdominal circumference (AC), and rump circumference (RC). The data included 96 pigs, with 739 sets of point cloud data before posture standardization transfer (including the original standard postures and non-standard postures) and 585 sets of point cloud data after transferring to standard postures. The green boxplots represent the relative errors of body sizes for the original postures, while the yellow boxplots represent the relative errors between the transferred standard posture and the original standard posture.

By observing the results of body length, body width, body

abdominal circumference. However, the changes in the hind legs in the nose-down posture were insignificant, resulting in relatively small errors in hindquarter height and rump circumference measurements. To sum up, the degree of lowering head affects the measurements of body height (front), thoracic circumference, and abdominal circumference.



height, and girth calculations, it can be seen that after posture standardization transfer, upper and lower limits and median have smaller errors compared to those before posture standardization transfer, indicating a better fitness to the standard posture, especially for body length, body width, and body height (front). This is because in posture standardization transfer, the parameters of body length, body width, and body height are the main focus. Therefore, the more skeleton joint points are available for the head and body, the better the transfer effect and the smaller the measurement errors. According to our research, the measurements of both thoracic circumference and abdominal circumference showed good results. In the measurement of thoracic circumference, different standing postures of the same pig, such as walking or standing, lead to different lengths of the fitted ellipse. The key point for abdominal circumference is the midpoint between the key points for body width (front) and body width (back). In the standard and

non-standard postures of a pig, the back of a pig arches when the pig looks ahead or lowers its head, resulting in an overestimated measurement of abdominal circumference. In our experiments, the measurement results of body width (back) and rump circumference did not show significant difference compared to the other parameters. This is mainly attributed to the fact that a pig tends to arch its back, with its rump located at the bottom of the arch. Since there are fewer skeleton joint points in the rump region, posture standardization transfer results in larger errors in body width (back) and rump circumference measurements, indicating less emphasis on the posture standardization transfer of the rump.

Table 2 shows the comparison of body size errors before and after posture standardization transfer, with the original standard

posture as a reference. It can be observed that after posture standardization transfer, the mean relative errors of body parameters decreased. The relative errors of body length, body width, and front height decreased significantly, with the average and maximum relative errors reduced by half. However, the mean relative errors of body height (back), thoracic circumference, abdominal circumference, and rump circumference, although reduced, are still relatively large. This is associated with the insufficient consideration of the correlation between the abdomen and rump in the posture standardization transfer, and this can also be attributable to the robustness of the point cloud completion algorithm for girth measurement and the automatic key point localization algorithm for body size measurement.

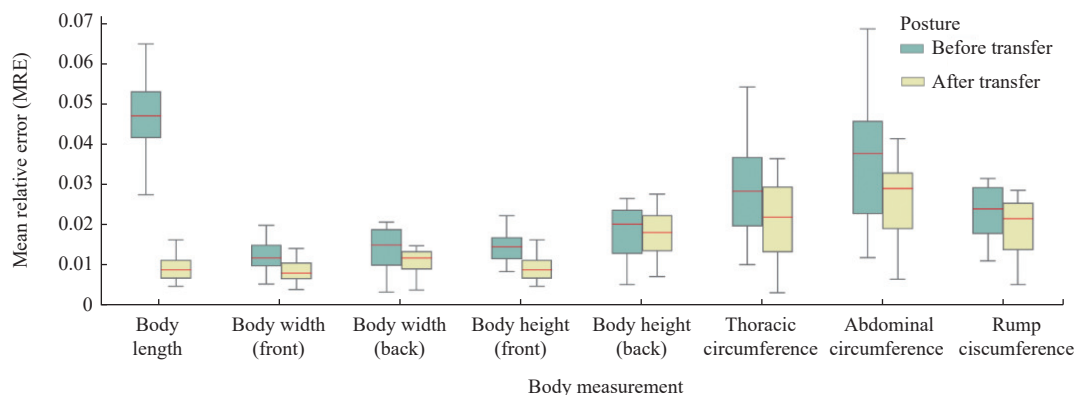


Figure 17 Mean relative errors for body size measurements of pigs

**Table 2 Comparison of body measurement errors between the transferred posture and the original standard posture before and after posture standardization transfer (%)**

Body size	Before posture standardization transfer		After posture standardization transfer	
	Mean relative error	Maximum relative error	Mean relative error	Maximum relative error
Body length	4.71	6.49	0.89	2.22
Body width (front)	1.19	2.37	0.76	1.33
Body width (back)	1.31	2.11	1.0	1.43
Body height (front)	1.43	3.21	0.89	2.22
Body height (back)	1.74	2.64	1.7	2.73
Thoracic circumference	2.8	5.42	2.03	3.61
Abdominal circumference	3.61	8.6	3.37	2.29
Rump circumference	2.24	3.17	1.89	2.85

In summary, the posture standardization transfer method proposed in this study has achieved encouraging results. In posture standardization transfer based on skeleton joint points, not only can the transformation from non-standard postures to standard postures be achieved, but also the localization of key points and curve fitting are improved, effectively reducing the errors in body size measurements.

#### 4 Discussion

The proposed method of pig point cloud skeleton extraction-based posture standardization transfer addresses the issue of measurement errors caused by different pig postures. By establishing the pig point cloud skeleton model and using the 3D point cloud skeleton as a proxy, the posture standardization transfer is achieved through weight binding of the point cloud skeleton and local point cloud rotation. Compared to existing posture

standardization transfer methods, the method proposed in this article neither relies on the topological structure of the mesh model nor requires vertex correspondence between source postures and target postures. Instead, our method directly processes the original pig point cloud data, remaining faithful to the collected pig point cloud data. According to the research results, the CD and MAE were 0.689 and 0.998, respectively, manifesting both the effectiveness and the robustness of our transfer method. Unlike methods that involve regression analysis and prediction based on a large amount of data, our method does not require extensive data for prediction, thus reducing prediction inaccuracies.

As for the comparison of body size measurement results, subjective factors can be avoided, as can potential inaccuracies introduced by human measurement, by using one body size calculation method for both the standard and non-standard postures of the same pig. The experimental results demonstrate that posture standardization transfer can effectively improve the accuracy of body size measurements. Compared to non-standard postures without posture standardization transfer, the average relative errors of the transferred standard posture are reduced to varying degrees, with body length, body width, body height (front), thoracic circumference, and abdominal circumference producing satisfactory transfer results.

Our method has some limitations. One restriction is that we did not establish a universal standard posture, so the goal of posture standardization transfer is not to make the pig posture exactly the same as the standard posture but to make it close to the standard posture as much as possible. Additionally, the pig legs were not included in the transfer process because their influence on the measurements is relatively limited in our model. Although the skeletal joint points of the legs remain unchanged during the posture standardization transfer, the overall changes in the pig body point cloud affect the measurements of body width, body height, and girth

to some extent.

The research focus of this study is on pig point cloud posture transfer, and a more detailed comparison of posture standardization transfer can be seen in [Figures 18 and 19](#). Future work will be required for further improvements; for instance, the transfer of the pig legs will be taken into account to enhance measurement accuracy. Currently, the emphasis is on point cloud posture transfer,

but no end-to-end network model is available for point cloud posture transfer. Following the proposed approach in this study, we will make more efforts to achieve point cloud posture transfer by resorting to neural networks. In the research field of animal body size measurements, the application can be extended to more datasets and improved for different animal body parts by optimizing the skeleton extraction and posture standardization transfer methods.

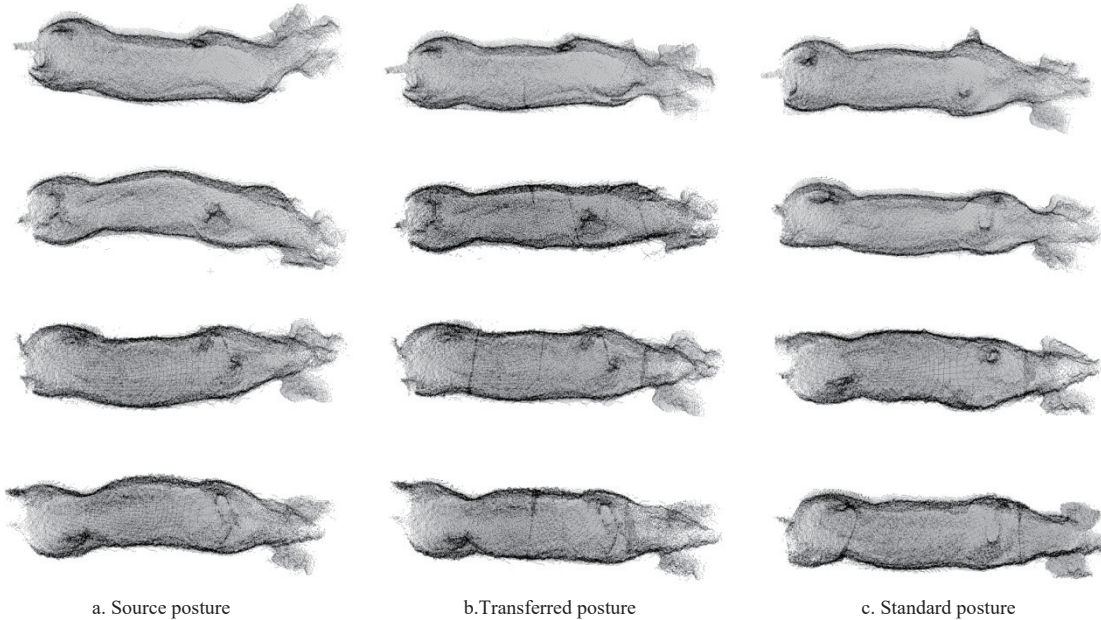


Figure 18 Comparisons of pig posture transfer (top view)

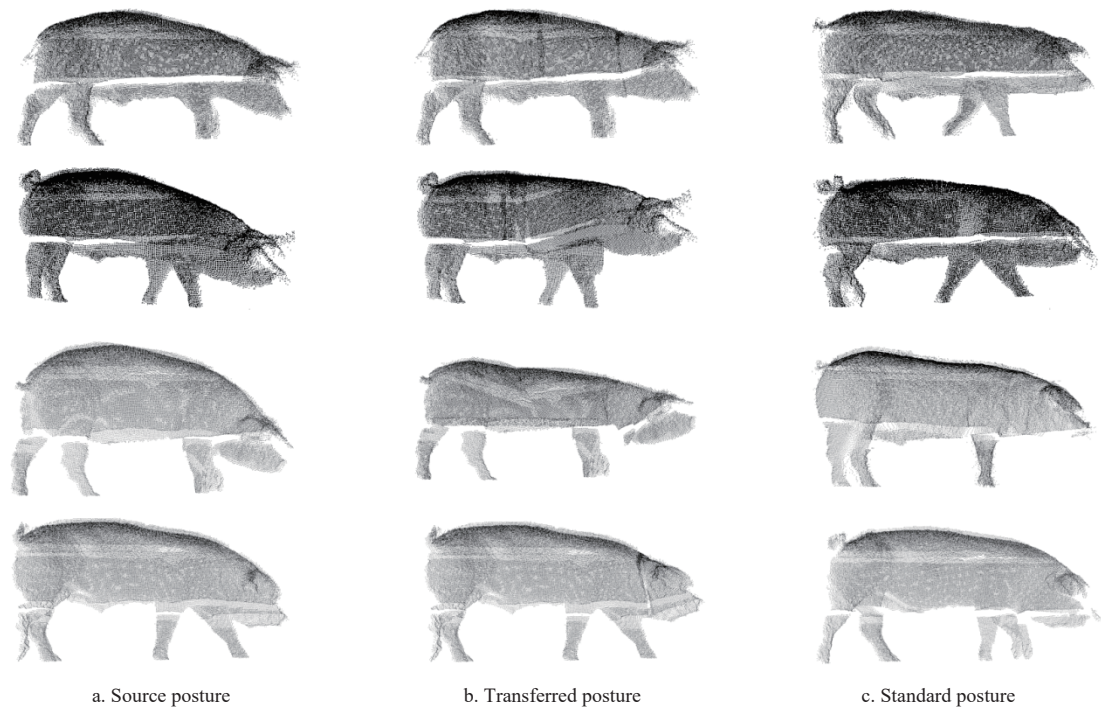


Figure 19 Comparisons of pig posture transfer (side view)

## 5 Conclusions

To handle the problem of inaccurate key point localization and algorithm robustness caused by different pig postures in automatic body size measurement based on point cloud data, we propose a posture standardization transfer method based on pig skeleton extraction models to transfer non-standard pig postures to standard

pig postures for further body size measurement. The main conclusions are summarized as follows:

(1) The pig skeleton extraction model based on point clouds can accurately describe pig postures. Although there are differences in the skeleton joint point vector sets between standard postures and non-standard postures, posture standardization transfer can be implemented through local point cloud rotation in non-standard

postures such as L-shaped, C-shaped, and nose-down postures, hence accurate point cloud data of pigs in standard postures can be generated.

(2) By comparing the experimental findings between non-standard postures and those of the original standard posture of the same target pig, the body size measurement results reveal that the average relative errors were 4.71% for body length, 1.19% for body width (front), 1.31% for body width (back), 1.43% for body height (front), 1.74% for body height (back), 2.8% for thoracic circumference, 3.61% for abdominal circumference, and 2.24% for rump circumference. These results indicate that the body size parameters in non-standard postures exhibit higher fluctuations, reflecting the influence of pig postures on the accuracy and stability of body size measurements. When comparing the results of the transferred posture with those of the original standard posture following posture standardization transfer and body size measurement, the average relative errors for body length, body width (front), body width (back), body height (front), body height (back), thoracic circumference, abdominal circumference, and rump circumference were 0.89%, 0.76%, 1%, 0.89%, 1.7%, 2.03%, 3.37%, and 1.89%, respectively. The parameters with the most significant impact on body size errors follow the descending order of: body length, body height (front), body width (front), body width (back), abdominal circumference, thoracic circumference, rump circumference, and body height (back).

## Acknowledgements

The authors thank Guangdong Wens Foodstuff Group Co., Ltd. for providing us with materials to conduct the experiments. The project was financially supported by the National Key R&D Program (2023YFD1300202), National Natural Science Foundation of China (Grant No. 32172780), Key Laboratory of Smart Agricultural Technology in Tropical South China, National Engineering Research Center for Breeding Swine Industry, and Guangdong Engineering Technology Research Center for Agricultural Farming Internet of Things.

## References

- Li G X, Liu X L, Ma Y F, Wang B B, Zheng L H, Wang M J. Body size measurement and live body weight estimation for pigs based on back surface point clouds. *Biosystems Engineering*, 2022; 218: 10–22.
- Qiao Y L, Kong H, Clark C, Lomax S, Su D, Eiffert S, et al. Intelligent perception for cattle monitoring: A review for cattle identification, body condition score evaluation, and weight estimation. *Computers and Electronics in Agriculture*, 2019; 185: 106143.
- Cominotto A, Fernandes A F A, Dorea J R R, Rosa G J M, Ladeira M M, van Cleef E H C B, et al. Automated computer vision system to predict body weight and average daily gain in beef cattle during growing and finishing phases. *Livestock Science*, 2020; 232: 103904.
- Nir O, Parmet Y, Werner D, Adin G, Halachmi I. 3D Computer-vision system for automatically estimating heifer height and body mass. *Biosystems Engineering*, 2018; 173: 4–10.
- Hemsworth P H. Key determinants of pig welfare: Implications of animal management and housing design on livestock welfare. *Animal Production Science*, 2018; 58(8): 1375–1386.
- Statham P, Hannuna S, Jones S, Campbell N, Colborne G R, Browne W J, et al. Quantifying defence cascade responses as indicators of pig affect and welfare using computer vision methods. *Scientific Reports*, 2020; 10(1): 1–13.
- Condotta I C F S, Brown-Brandl T M, Pitla S K, Stinn J P, Silva-Miranda K O. Evaluation of low-cost depth cameras for agricultural applications. *Computers and Electronics in Agriculture*, 2020; 173: 105394.
- Pezzuolo A, Guarino M, Sartori L, González L A, Marinello F. On-barn pig weight estimation based on body measurements by a Kinect v1 depth camera. *Computers and Electronics in Agriculture*, 2018; 148: 29–36.
- Ruchay A, Kober V, Dorofeev K, Kolpakov V, Miroshnikov S. Accurate body measurement of live cattle using three depth cameras and non-rigid 3-D shape recovery. *Computers and Electronics in Agriculture*, 2020; 179: 105821.
- Wang X J, Dai B S, Wei X L, Shen W Z, Zhang Y G, Xiong B H. Vision-based measuring method for individual cow feed intake using depth images and a Siamese network. *Int J Agric & Biol Eng*, 2023; 16(3): 233–239.
- Du A, Guo H, Lu J, Su Y, Ma Q, Ruchay A, et al. Automatic livestock body measurement based on keypoint detection with multiple depth cameras. *Computers and Electronics in Agriculture*, 2022; 198: 107059.
- Guo H, Wang K, Su W, Zhu D H, Liu W L, Xing C, et al. 3D scanning of live pigs system and its application in body measurements. *International Archives of the Photogrammetry, Remote Sensing and Spatial Information Sciences*, 2017; pp.211–217. doi: [10.5194/isprs-archives-XLII-2-W7-211-2017](https://doi.org/10.5194/isprs-archives-XLII-2-W7-211-2017).
- Kwon K, Mun D. Iterative offset-based method for reconstructing a mesh model from the point cloud of a pig. *Computers and Electronics in Agriculture*, 2022; 198: 106996.
- Salau J, Haas J H, Junge W, Thaller G. A multi-Kinect cow scanning system: Calculating linear traits from manually marked recordings of Holstein-Friesian dairy cows. *Biosystems Engineering*, 2017; 157: 92–98.
- Hu H, Yu J C, Yin L, Cai G Y, Zhang S M, Zhang H. An improved PointNet++ point cloud segmentation model applied to automatic measurement method of pig body size. *Computers and Electronics in Agriculture*, 2023; 205: 107560.
- Yin L, Cai G Y, Tian X H, Sun A D, Shi S, Zhong H J, et al. Three dimensional point cloud reconstruction and body size measurement of pigs based on multi-view depth camera. *Transactions of the CSAE*, 2019; 35(23): 201–208.
- Han H, Xue X L, Li Q F, Gao H F, Wang R, Jiang R X, et al. Pig-ear detection from the thermal infrared image based on improved YOLOv8n. *Intell Robot*, 2024; 4(1): 20–38.
- Le Cozler Y, Allain C, Xavier C, Depuille L, Caillot A, Delouard J M, Delattre L, et al. Volume and surface area of Holstein dairy cows calculated from complete 3D shapes acquired using a high-precision scanning system: Interest for body weight estimation. *Computers and Electronics in Agriculture*, 2019; 165: 104977.
- Nguyen A H, Holt J P, Knauer M T, Abner V A, Lobaton E J, Young S N. Towards rapid weight assessment of finishing pigs using a handheld, mobile RGB-D camera. *Biosystems Engineering*, 2023; 226: 155–168.
- Liu D, He D J, Norton T. Automatic estimation of dairy cattle body condition score from depth image using ensemble model. *Biosystems Engineering*, 2020; 194: 16–27.
- Martins B M, Mendes A L C, Silva L F, Moreira T R, Costa J H C, Rotta P P, et al. Estimating body weight, body condition score, and type traits in dairy cows using three dimensional cameras and manual body measurements. *Livestock Science*, 2020; 236: 104054.
- Miller G A, Hyslop J J, Barclay D, Edwards A, Thomson W, Duthie C A. Using 3D imaging and machine learning to predict liveweight and carcass characteristics of live finishing beef cattle. *Frontiers in Sustainable Food Systems*, 2019; 3: 30.
- Li Z, Mao T T, Liu T H, Teng G H. Comparison and optimization of pig mass estimation models based on machine vision. *Transactions of the CSAE*, 2015; 31(2): 155–161. (in Chinese)
- Yin L, Zhu J M, Liu C X, Tian X H, Zhang S M. Point cloud-based pig body size measurement featured by standard and non-standard postures. *Computers and Electronics in Agriculture*, 2022; 199: 107135.
- Li J W, Ma W H, Bai Q, Tulpan D, Gong M L, Sun Y, et al. A posture-based measurement adjustment method for improving the accuracy of beef cattle body size measurement based on point cloud data. *Biosystems Engineering*, 2023; 230: 171–190.
- Luo X Y, Hu Y H, Gao Z C, Guo H, Su Y. Automated measurement of livestock body based on pose normalisation using statistical shape model. *Biosystems Engineering*, 2023; 227: 36–51.
- Lu J, Guo H, Du A, Su Y, Ruchay A, Marinello F, et al. 2-D/3-D fusion-based robust pose normalisation of 3-D livestock from multiple RGB-D cameras. *Biosystems Engineering*, 2022; 223: 129–141.
- Shi S, Yin L, Liang S H, Zhang H J, Tian X H, Liu C X, et al. Research on 3D surface reconstruction and body size measurement of pigs based on multi-view RGB-D cameras. *Computers and Electronics in Agriculture*, 2020; 175: 105543.
- Huang H, Wu S H, Cohen-Or D, Gong M L, Zhang H, Li G Q, et al.  $L_1$ -medial skeleton of point cloud. *ACM Transactions on Graphics*, 2013; 35(4): 65.
- Fitzgibbon A, Pilu M, Fisher R B. Direct least square fitting of ellipses. *IEEE Transactions on Pattern Analysis and Machine Intelligence*, 1999; 21(5): 476–480.